Seismic and stratigraphic characterization of karstogenic horizons in a sequence of carbonate deposits: Example of the Dogger limestones of the Poitou threshold

Caractérisation sismique et stratigraphique des horizons karstogènes dans une séquence de dépôts carbonatés : exemple des calcaires du Dogger du seuil du Poitou

Thierry Gaillard[*,1], *Mickaël* Moreau[1], *Jean-Luc* Mari[2]

[1] CPGF HORIZON, 49 avenue Franklin Roosevelt, 77210 Avon

[2] Sorbonne Université, Paris, France

Abstract. The Deffend Hydrogeological Experimental Site (HES), near Poitiers, has been the site of numerous studies that have shown that the Bajocian and Aalenian limestones were modified by the horizontal development of multiple karstification planes. These investigations have demonstrated the occurrence of stacked circulation. The origin of the structures that generated these sub-horizontal flows has not been specifically explained. Geophysical investigations were conducted at the site, both at the surface (3D seismic) and in wells (vertical seismic profile (PSV) and acoustic logging). Comparison of the geophysical data, mainly acoustic logs, and a stratigraphic interpretation of cuttings and borehole wall imaging makes it possible to propose a coherent karstogenesis scheme that does not involve tectonic constraints. This article offers an explanation based on gaps recorded in the sequence of Dogger deposits. The karstogenic horizons are linked to sedimentary discontinuities that geologists have identified on the Poitou threshold.

Résumé. Le site Expérimental hydrogéologique (SEH) du Deffend, près de Poitiers, a fait l'objet de nombreuses études qui ont démontré que les calcaires du Bajocien et de l'Aalénien étaient affectés par le développement

* Corresponding author: tgaillard@cpgf-horizon.fr

horizontal de plusieurs plan de karstification. Ces investigations ont démontré l'existence de circulations étagées. L'origine des structures permettant ces écoulements subhorizontaux n'a pas fait l'objet d'explications particulières. Le site a fait l'objet d'investigations géophysiques de surface (sismique 3D) et de puits (profil sismique vertical (PSV) et diagraphie acoustique). La comparaison des données géophysiques, principalement des logs acoustiques, et d'une interprétation stratigraphique des cuttings et imageries de parois permet de proposer un schéma de karstogénèse cohérent, ne faisant pas intervenir les contraintes tectoniques. Cette publication propose une explication fondée sur l'enregistrement de lacunes dans la séquence de dépôts du Dogger. Ces horizons karstogènes sont liés à des discontinuités sédimentaires bien identifiées sur le seuil du Poitou par les géologues.

Introduction

The Poitou threshold is located between the Aquitaine and Paris basins (France), where two aquifers are present: the *Lias* aquifer, called infra-*Toarcian* because the *Toarcian* marls form its roof, and the *Dogger* aquifer, called supra-*Toarcian*, in which the marls form the aquifer's impermeable base. The nature of flows in the supra-*Toarcian* aquifer have been discussed since the nineteenth century and the establishment of the first drinking water supply system. Two scenarios have been commonly used for exploration and wellhead protection.

The first and oldest scenario is based on observations made by the forest engineer between 1886 to 1889 during the excavation of the tunnel designed to collect the Fleury springs to supply the city of Poitiers. During construction, workers observed "three superimposed aquifers" in the *Bajocian* limestones [1]. Indeed, as the canal was dug, overlying water inlets were encountered above the contact with the *Toarcian* marls. This project therefore showed that water was circulating in superimposed horizontal networks.

The second explanation was exposed by Professor Welsh, geologist at the University of Poitiers, who proposed dry valleys as axes of subsurface drainage to springs and thus partly explains the location of springs [2]. Vertical fracturing in valleys as a result of decompression of the limestone massif explains this type of drainage.

The Poitiers Hydrogeological Experimental Site (HES) is therefore of crucial interest for studying groundwater motion and investigating the presence of stacked aquifers. The IC2MP/Hydrasa team (UMR CNRS 7285), as part of the National Network of Hydrogeological Sites (SNO H+), and the "WATER" programs of the Poitou-Charentes region (CPER 2002-2006 and 2007-2013) conducted studies on the plateau on a piezometric divide of the supra-*Toarcian* aquifer.

Located 2 km east of the University of Poitiers campus, the HES covers an area of 12 hectares (Fig. 1).The experimental set-up now includes 35 boreholes, including two vertical core drills (C1 and C2) and two inclined core drills (C3 and C4). All boreholes cross the entire Dogger aquifer and are arranged in a regular grid within a 210 × 210 m square (Fig. 2).

The authors investigated the site from the surface via hybrid seismic imaging (3D seismic survey) and in boreholes via Full Wave form Acoustic Logging (FWAL) and Vertical Seismic Profiles (VSP).

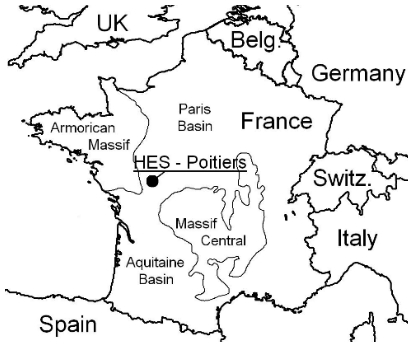

Fig. 1. Location of the Hydrogeological Experimental Site (HES): Deffend, France [3].

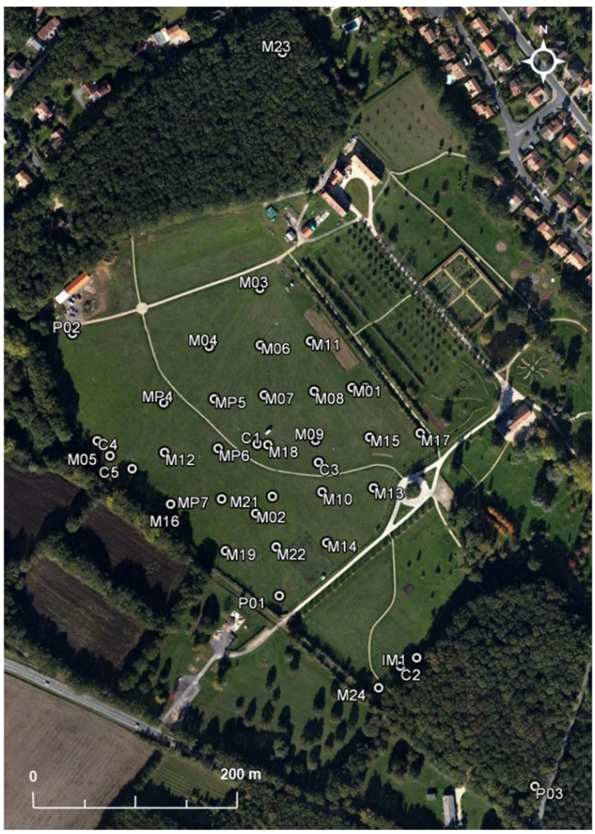

Fig. 2. Location of boreholes at the Deffend site [3].

1 Geophysical investigations

The HES has a total extent of approximately 300×300×150 m^3. Geophysicists designed a 3-D seismic survey [3], implemented with light seismic spreads, to obtain a 3-D block in depth using the time – versus depth relationship obtained by VSP recorded in borehole C1 (figure 3b). The block extends 240 m in the in-line direction and 300 m in the crossline direction [3, 4]. Structural interpretation of the 3D block leads to the conclusion that the stratigraphy is nearly horizontal with a dip of 1 degree to the west. Consequently, the site has no tectonic features with vertical displacement. The 3D seismic block was converted into a 3-D pseudo velocity block using acoustic velocity logs as constraints and then into a pseudo-porosity block that reveals three high-porosity, presumably water-producing layers, at depths of 35-40, 85-87 and 110-115 m [4, 5].The 85-87 m- layer is the most porous, with bodies of porosity greater than 30%; this porous layer represents the major karstic part of the reservoir (figure 3a).

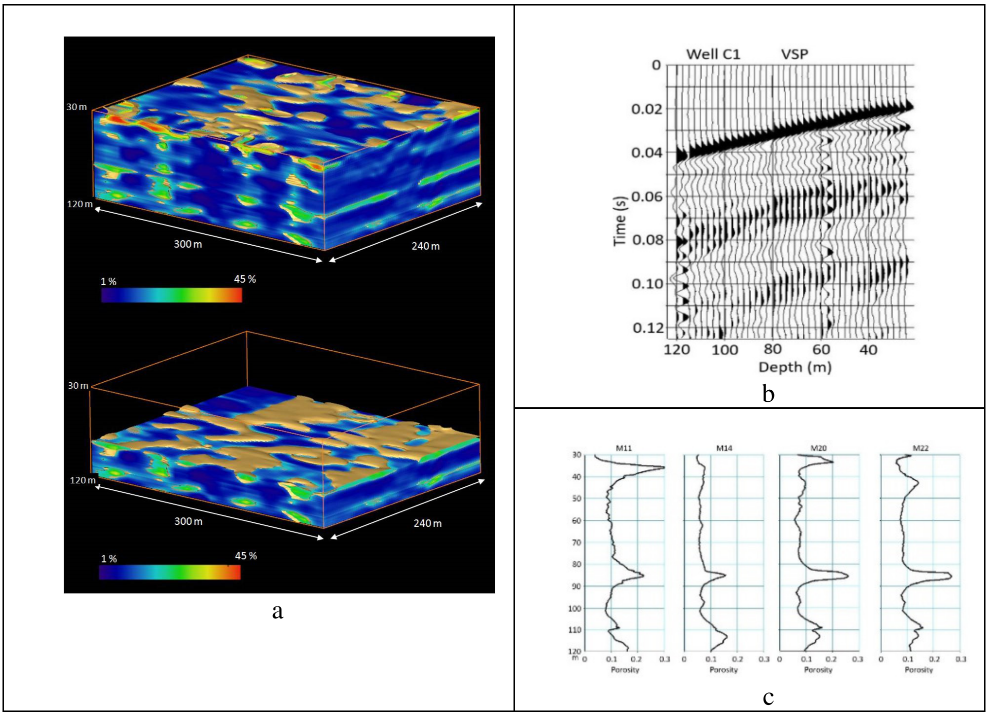

Fig. 3. Geophysical investigations at the HES site. After [5]
a: pseudo porosity block in the 30 – 120 m depth interval (top) and in the 85 – 120 m depth interval (bottom); b: VSP recorded at well C1; c: porosity seismic logs at wells M11, M14, M20 and M22.

In 2014, full waveform acoustic data were recorded in nine wells (C1, M03, M05, M11, M13, M14, M20, M22, and MP7). Wells M11, M14 , M20 and M22 were selected for seismic and stratigraphic characterization of karstogenic horizons, (figure 2). Figure 3c shows the porosity seismic logs extracted from the 3D block (figure 3.a) at the locations of the four boreholes. The major karstic level in the 80 – 90 m depth interval is clearly visible on all logs.

Acoustic logging at the HES site was done with an acoustic probe, which is a flexible monopole tool containing a magnetostrictive transducer as a source and a pair of far receivers (3 and 3.25 m lag-distances (offsets) beneath the source). Acoustic data were recorded in the 1 – 20 kHz frequency band. The acoustic data are conventionally displayed as constant offset sections. Examples of constant offset sections recorded in boreholes M14 and M20 are shown in figure 4. Compared with seismic data, the vertical resolution of acoustic logging is very high, on the order of 10 cm, but the lateral investigation is limited to a few tens of centimeters around the borehole. Acoustic data were processed to obtain acoustic logs including a P-wave velocity log and a P-wave amplitude log (figures 5a and 5b). Processing based on singular value decomposition was applied to the constant offset acoustic sections to compute a specific attribute, called the *Noise/Signal detector* or *K-index* (figure 5c), which was used to detect karstic levels [6]. The *K-index* attribute (figure 5c) is the product of 3 normalized terms: an amplitude term (1- Amp(z)/AmpMax, with Amp(z) defined as the acoustic amplitude at depth z and AmpMax the highest acoustic amplitude), a correlation term (1- Cor(z)/CorMax, where Cor(z) is the correlation coefficient at depth z and CorMax is the highest correlation coefficient), and a velocity term (1- VP(z)/VPMax, where VP(z) is equal to the P-wave velocity at depth z and VPMax equals the highest P-wave velocity) [6]. Integration versus depth of the K-index from the bottom to the top of the well was done to mimic a flowmeter (acoustic flow detector or A-flow, figure 5d).

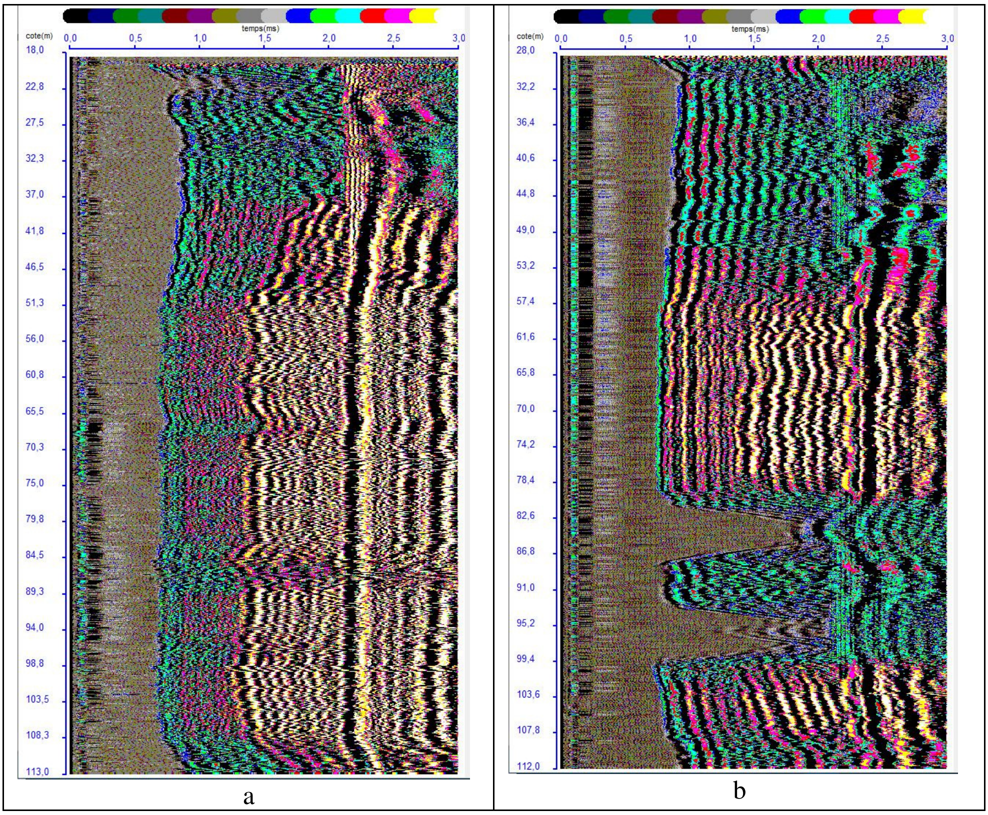

Fig. 4. Acoustic sections recorded at boreholes M14 (a) and M20 (b).

On the acoustic section recorded in borehole M14 (figure 4a), refracted P-waves appear in the 0.5-1.2 ms time interval, converted refracted S-waves and pseudo-Rayleigh waves in the 1.2- 2 ms time interval, and Stoneley wave in the 2-3 ms time interval. The logging distinguishes:

- The 22 - 38 m depth interval, where only refracted P-waves and Stoneley waves are recorded, indicating a slow formation. We note the presence of fluid waves.
- The 38-110 m depth interval of homogeneous profile with a high signal to noise ratio; all acoustic waves (refracted P-wave, converted refracted S-wave, and Stoneley wave) are visible and of high amplitude, indicating a compact formation. No fluid waves are visible. However, in the 85 – 88 m depth interval, we note a very weak attenuation of the various waves, which is confirmed by small decreases of both the P-wave velocity log and the amplitude log (figures 5a and 5b).

Analysis of the acoustic data (figure 5c) shows a small but significant increase of karstic body indicators in the 85 – 90 m depth interval, suggesting the presence of a karstic feature filled with sediments such as shale. However, no flow is present.

The acoustic section recorded in borehole M20 (figure 4b) shows:

- In the 30 – 58 m depth interval, an acoustically slow formation where only refracted P-waves and Stoneley waves propagate.
- In the 58 – 80 m depth interval, an acoustic fast formation where refracted P-waves, converted refracted S-waves and Stoneley waves propagate, indicating a compact geological formation.
- A karstic unit in the 80 – 100 m depth interval, characterized by a strong attenuation of refracted P-waves (figure 5b) and Stoneley waves. In the interval, we can infer the presence of fluid waves, indicating the presence of flow (figure 5d).
- In the 100 – 110 m depth interval, an acoustically fast formation where refracted P-waves, converted refracted S-waves and Stoneley waves propagate, indicating a compact geological formation.

The acoustic logs (figures 5b and 5c) clearly show that the karstic unit is composed of two karstic levels at depths of 82 – 85 m and of 93 – 100 m. The two levels have been confirmed by OPTV (optical televiewer) logs.

Figure 5 shows the distribution of karstic bodies detected by acoustic logging in boreholes M11, M14, M20 and M22.

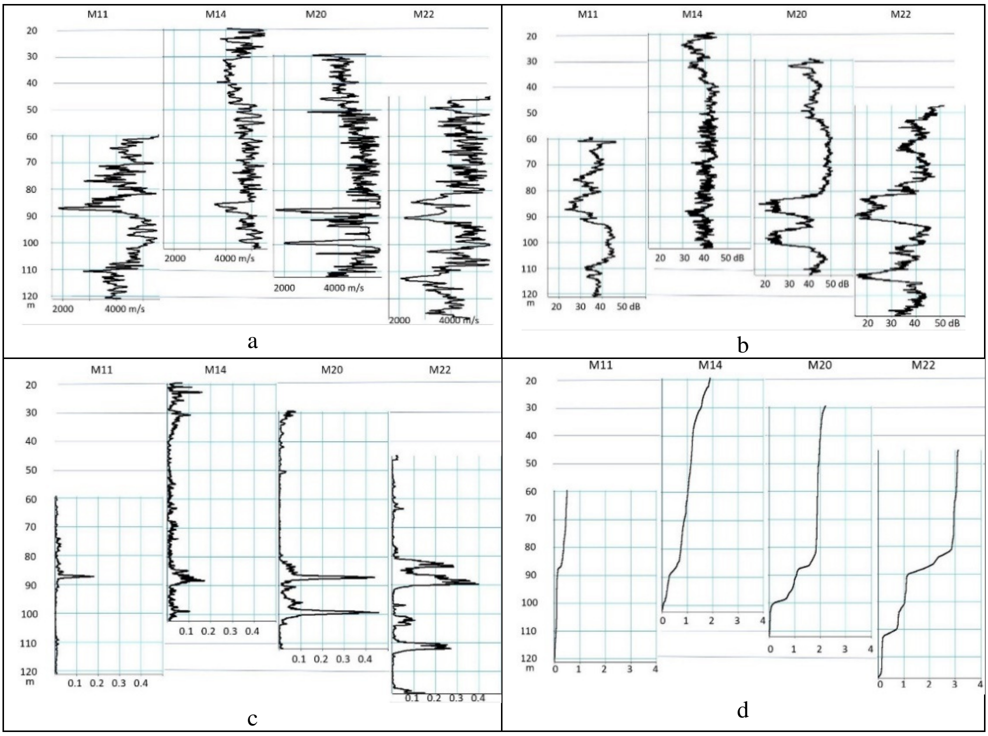

Fig. 5. Acoustic logs in boreholes M11, M14, M20 and M22.
a: acoustic velocity logs, b: acoustic amplitude logs, c: K-index logs , d: A- flow logs. Karstic bodies and flows are detected in the 80 – 90 m and 110 – 115 m depth intervals.

2 Stratigraphic setting

The stratigraphy of the Poitou threshold was defined in detail in the 1970s. The central region has been called the Pictave platform [7, 8, 9]. Geologists have identified 107 ammonite biozones in the *Sinemurian* to the *Oxfordian* [10, 8]. Gabilly understood the importance of considering major sedimentary discontinuities and depositional facies in the study of stratigraphy [7]. In contrast to earlier geologists, Gabilly observed regional-scale discontinuities [11]. The Poitou Threshold series was thus revised and divided into 13 sequences separated by discontinuities. The series was presented in 1974 during an excursion to the Poitou Threshold organized by Gabilly and Cariou. For the *Dogger*, the regional sequences were defined as follows [8] :

- The upper sequence of the Terminal *Toarcian* and *Aalenian*,
- The Lower *Bajocian* sequence,
- The Upper *Bajocian* sequence, which includes the base of the *Bathonian*,
- The Lower *Bathonian* sequence,
- The Upper *Bathonian* sequence,
- The *Callovian* sequence.

This division was later used in theses written at Poitiers university [12] [13] [14] [15] and on the 1/50000 geological maps of Poitiers, Chauvigny, Lusignan, Gençay, Montmorillon and Civray. Discontinuities are numbered in a 1985 paper [16] as D1 to D33, from oldest to most recent. They correspond to gaps in ammonite horizons with durations estimated between 200 ka (5th order) to 1 Ma (D8, 4th order). Discontinuities followed by a suffix (D8bis) indicate discontinuities of one or two ammonite horizons noted by Mourrier [15] and Branger [14]. With these notation conventions, it is possible to describe the Pictave platform deposits as follows.

Two Aalenian depositional sequences are recognized in outcrop [13, 12, 9]. On the western side of the threshold, the first sequence ends with polypiers and large silicified wood fragments. The upper surface of the first sequence is a discontinuity between the *Bradfordensis* and *Gigantea* zones, named D6 by Gabilly et al. [16]. The second sequence, consisting of limestones with oncolites and oolites, ends with a landmark level of crinoidal limestones. The top is defined by the D7 discontinuity.

During the Bajocian, major gaps with erosional surfaces are evident in the sedimentary record of the Pictave Platform [17, 16, 18]. The first occurs at the Aalenian/Bajocian boundary (D7 according to [16], post *Concavum* according to [14]). The missing horizons are *Concavum* and especially *Discites*. Overlying sedimentation is marked by limestone pebbles sometimes encrusted with serpulidae [7, 13]. Discontinuity D8 is particularly noticeable in the field for its extent and flat morphology. It lies between the *Humphriesianum* (*Blagdeni* subzone) and *Niortense*, *Garantiana,* or *Parkinsoni* zones, depending on the size of the gap. It marks the transition from the Lower *Bajocian* to the Upper *Bajocian* (D8 by [16], post *Coronatum* according to [14]). The post-*Sauzei* discontinuity, identified around Poitiers as a flat surface marking the transition to the *Humphriesianum* zone, is here named D7bis to follow Gabilly's numbering. The post-*Subgaranti* discontinuity, also readily observable on the Pictave platform, is here named D8bis. Gabilly described it in the Montmidi cliff at Poitiers [19].

In the *Bathonian*, the subdivision that was adopted comprises three sequences [17]. Another important discontinuity recorded on the platform occurs at the top of the *Bajocian*, at the *Parkinsonia*/*Zigzag* boundary (D9). This discontinuity is marked by a continental influence from east of the platform, consisting of lacustrine green clays [15, 20] and the absence of the *Gonolkites* and *Bomfordi* horizons. Above this discontinuity, a fossiliferous benchmark (*Ctenostreon* stratum) provides evidence for a benthic environment. The Lower and Middle *Bathonian* boundary (D10) is a gap of the *Progracilis* zone, which may extend into the *Subcontractus* zone. Finally, the top of the *Bathonian* is marked by a major gap (D11) in the *Discus* zone of the *Bathonian* that continues into the Callovian (*Bullatus* horizon gap).

Using this stratigraphic framework, the authors aim to evaluate the concordance between discontinuities and positions of *Dogger* karstic levels.

3 Borehole study

3.1 Methodology

To study the discontinuities, the authors used core descriptions of SC1 and SC2 [21] and optical televiewers in each well. OPtical TeleViewer (OPTV) is a borehole logging technique that scans borehole walls to obtain a full 360° image. The authors used these images to identify depositional sequences and discontinuities. The method is based on the following steps:

1- Definition of OPTV facies: these are formations that appear homogeneous on imagery in terms of texture, sedimentary particles, and bench thickness; certain paleontological features also characterize these facies.
2- Location of depositional discontinuities within the regional framework.
3- Assigning sequences to a geological formation and an ammonite zone based on the division presented above and the discontinuity numbering established by Gabilly et al. [16].

Observation of cuttings and OPTV made it possible to define eight (8) facies. They are characterized as follows:

- Facies 1: meter-thick stratum of homogenous limestone, yellow in colour with black flint strata. Stratification is well marked, and bioturbation is limited to two horizons of dissolved shells.
- Facies 2: meter-thick stratum of homogenous limestone with disseminated black flint. Bioturbation is very noticeable, with vertical burrows.
- Facies 3: meter-thick beds with millimeter-thick laminae, strongly bioturbated at the top of each bed, giving it a pebble appearance (called potato bed by quarrymen).
- Facies 4 : decimeter-thick stratum of nodular limestone with *Trichites*; towards the base, the limestone appears marbled under the effect of intense bioturbation.
- Facies 5: non-bioturbated meter-thick stratum appearing much lighter in color and granular, often arranged in three (3) strata of oolite limestone about 1 m thick per stratum.
- Facies 6: facies remarkable for its black colour and the presence of centimeter- to decimeter-wide vacuoles. This formation has no visible stratification or identified paleontological evidence; this facies is related to dolomite in a reducing aqueous environment, as described by Mourrier [15].
- Facies 7: decimeter-thick grey chert (probably from silicified wood).
- Facies 8: bicoloured black/grey facies in centimeter-thick stratum with traces of silicified wood. Under scanning camera (OPTV), the base appears wavy (erosional flood boundary).

Figure 6 shows the facies and the primary biostratigraphic markers that were observed. Some facies appear several times in the depositional sequence.

https://doi.org/10.1051/e3sconf/202450405005

	Facies	Main markers
Facies 1	 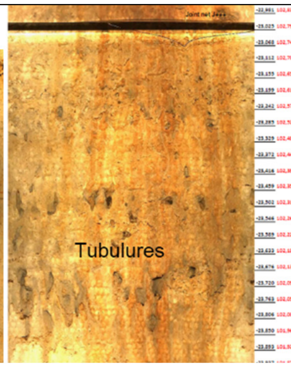	 Lumachel bivalves at base  *Ctenostreon* sp.
Facies 2	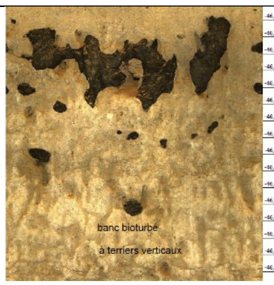 nodular facies	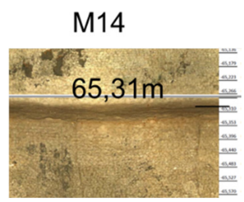 Discontinuity with clay deposit
Facies 3	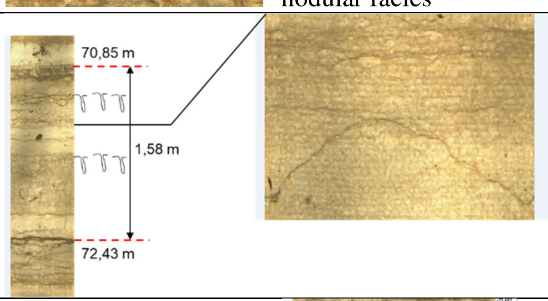	 Fine stratum (1-5 mm)
Facies 4	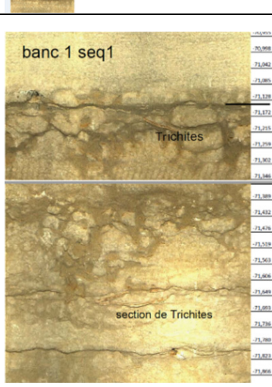 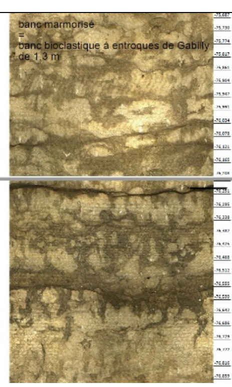 Burrowed strata	 Trichites sp. 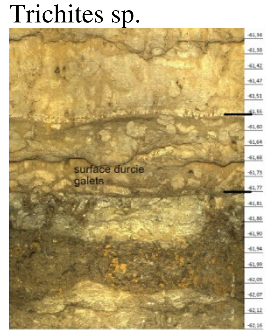 Potato facies

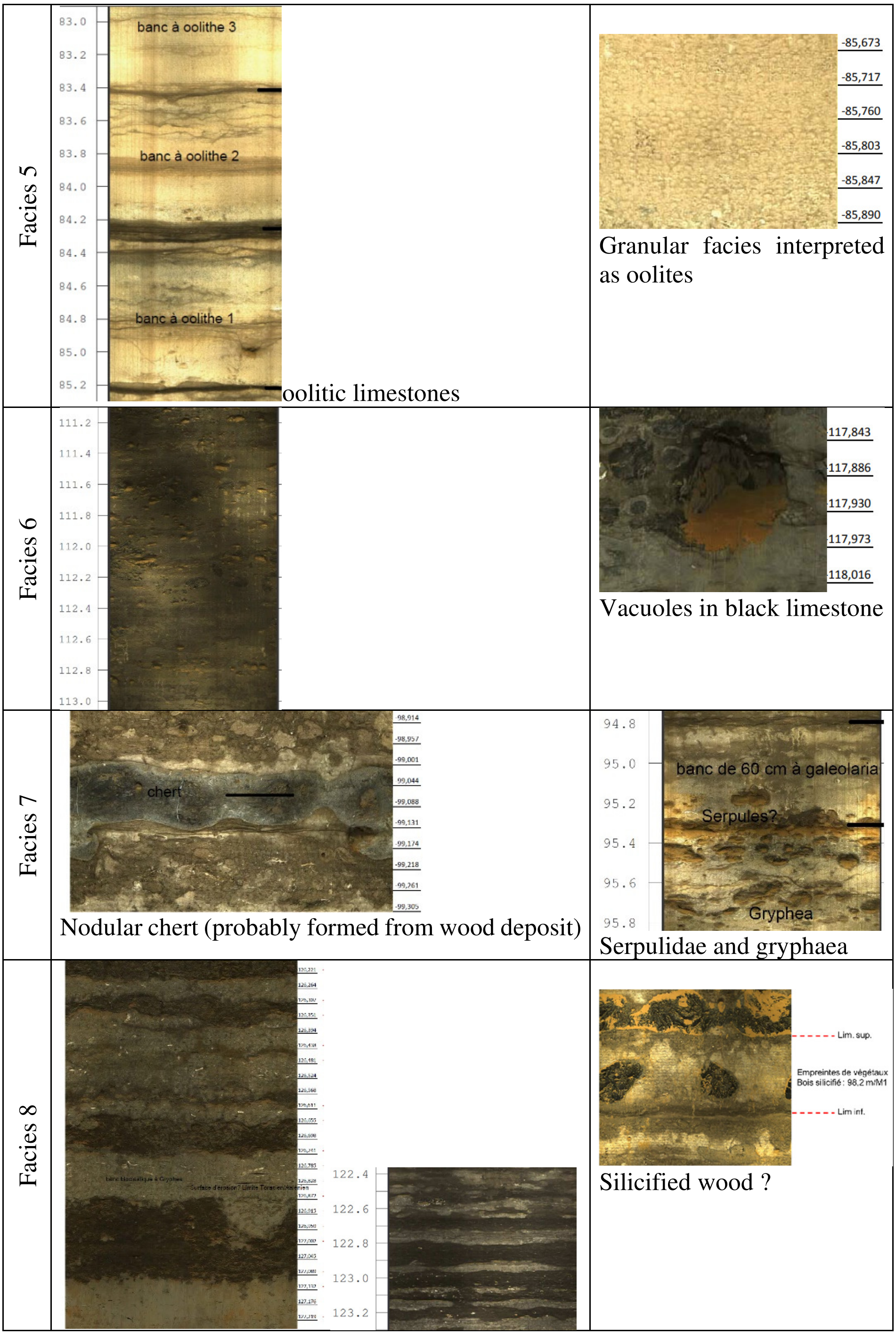

Fig. 6. Facies and bio-sedimentary markers.

3.2 Stratigraphical interpretation

Analysis of OPTV facies makes it possible to locate discontinuities and to characterize their depositional environments.

The top of facies 1 shows an important horizontal joint noted J+ on our surveys (M1, M10, and P2 boreholes). Below this joint, vertical bioturbation can be seen over 70 cm above a scattered flint bed. Two flint strata that mark the base of the flint bed can be seen in all boreholes. The joint is compared here to discontinuity D11. At the base of this sequence, a notable shell-bearing bed corresponds to large bivalves observed on cores [21]. A *Ctenostreon* test recovered from C4 cores led to this horizon being assigned to Gabilly's *Ctenostreon* stratum [19]. The joint at the base of this stratum therefore corresponds to discontinuity D9. The stratigraphic assignment thus corresponds to the Bathonian *sensus lato*.

Facies 2 begins above a first nodular facies bioturbated bed (potato stratum) and grades into facies 3 at various depths according to the borehole. The base of facies 3 consists of a coarse limestone bed with a hardened surface at the top and a very sharp joint at its base, highlighted by a deposit of black clay. The facies and bioturbation of facies 3 makes it possible to assign this bedding to the burrow beds of Montmidi cliff [19]. The two facies thus represent the Upper Bajocian, *Garantiana* and *Parkinsoni* zones, with the D8 discontinuity at the base and D8bis, as named here, at the top of the *Garantiana* zone [16].

The underlying facies 4 is easily correlated with the *Trichites* bedrock. A joint underlies its base. Facies 5 is highly variable in OPTV, and on the basis of its cuttings it was linked to Lower Bajocian oolitic limestone with sparry calcite cement. The transition from facies 4 to 5 thus corresponds to the transition from the *Laeviuscula* zone to the *Humphriesianum* zone.

A “new facies 4” appears below, marked at its base by a *serpulidae* bed. This bed is known as the *Galeolaria socialis* bed [13] [12] which is equivalent to discontinuity D7 of Gabilly et al. [16].

The underlying facies 6 is of diagenetic origin (dolomitization). Facies 6 alternates with facies 4, which is the primitive limestone. Facies 5 reappears at around 103 m and corresponds to a second oolitic event, known near Poitiers to belong to the late Aalenian depositional sequence. The authors have named this discontinuity D6bis. Below this discontinuity, the transition from facies 6 to 7 corresponds to discontinuity D6 at the base of the *Murchisonae* zone. A bioturbated undulating surface characterizes D6. Facies 8 represents the first sequence of the *Aalenian* stage.

4 Stratigraphic setting of geophysical horizons

To verify the hypothesis that karstogenesis is linked to stratigraphy at the “Le Deffend” site, the authors compared lithostratigraphic descriptions of several boreholes and the geophysical data available for these same boreholes. The comparison was first done using M14, then M20, M11, and C1. For M14, M20, and M11, the lithological description is based on optical logs (OPTV). In the case of C1, it was possible to visually describe the cores.

More specifically, the high-resolution optical imagery available from M14 facilitated a detailed description of the Aalenian, Bajocian, and Bathonian facies, as well as locating the stratigraphic discontinuities described by Welsh [11] and Mourrier and Branger [13]. The authors then compared the M14 facies depths and the stratigraphic discontinuity positions with the acoustic logs. The same search for relationships between stratigraphic discontinuities and geophysical data was then done in boreholes M20, M11, and C1 to validate the concordances identified in M14.

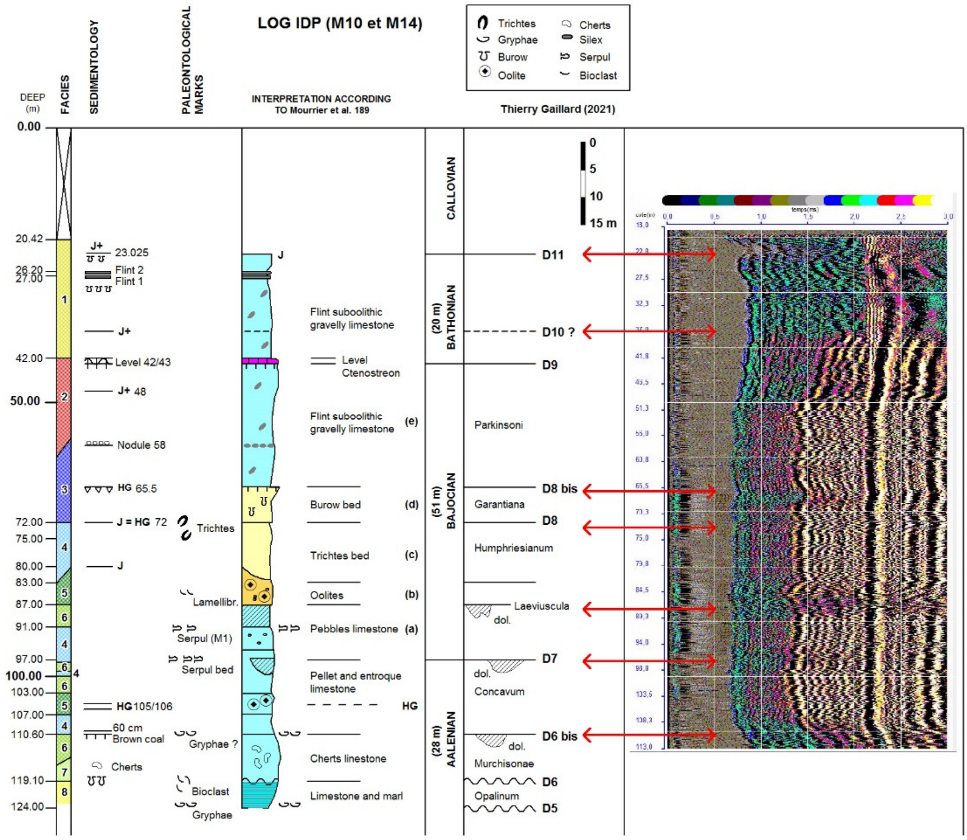

Fig. 7. Facies and stratigraphic interpretation compared with the acoustic section on M14.

Comparison between geological facies, their stratigraphic interpretation, and the acoustic data displayed as a constant offset section on M14 (see figure 7) shows:

- The concordance between discontinuity D10 and the base (37 m) of a domain defined as an acoustically slow formation.
- The concordance between the very low attenuation depths of various waves and depths of the following stratigraphic discontinuities:
  - D11 at 23 m (boundary between Bathonian and Callovian).
  - D8bis at 65 m (boundary between the *Garantiana* biozone and the *Parkinsoni* biozone in the *Bajocian*).
  - D8 at 72 m (boundary between the *Humphriesianum* biozone and the *Garantiana* biozone in the *Bajocian*).
  - "*Laeviuscula*" discontinuity at 87 m (stratigraphic boundary between the *Sowerbyi* biozone and the *Sauzei* biozone in the *Bajocian*).
  - D7 at 97 m (boundary between *Aalenian* and *Bajocian*).
  - D6bis at 110 m (boundary between the *Murchisonae* biozone and the *Concavum* biozone in the *Aalenian*).

The depth of low attenuation zones of the various waves is consistent with dolomitized zones that are limited by discontinuities D6bis, D7, and *Laeviuscula* at their roof. Discontinuity D9 (transition from Bajocian to Bathonian) was not observed on the acoustic logging.

The accurate recognition of the stratigraphic discontinuity was facilitated by the limited development of karst conduits in M14. However, Figure 8 shows a comparison among the lithostratigraphic log of M14, the K-index, and the A-flow index. These indices, obtained by acoustic log processing, make it possible to determine the positions of karstic conduits correlated with stratigraphic discontinuities D11, *Laeviuscula,* and D7. The strongest karst index is located at the *Laeviuscula* discontinuity in this borehole.

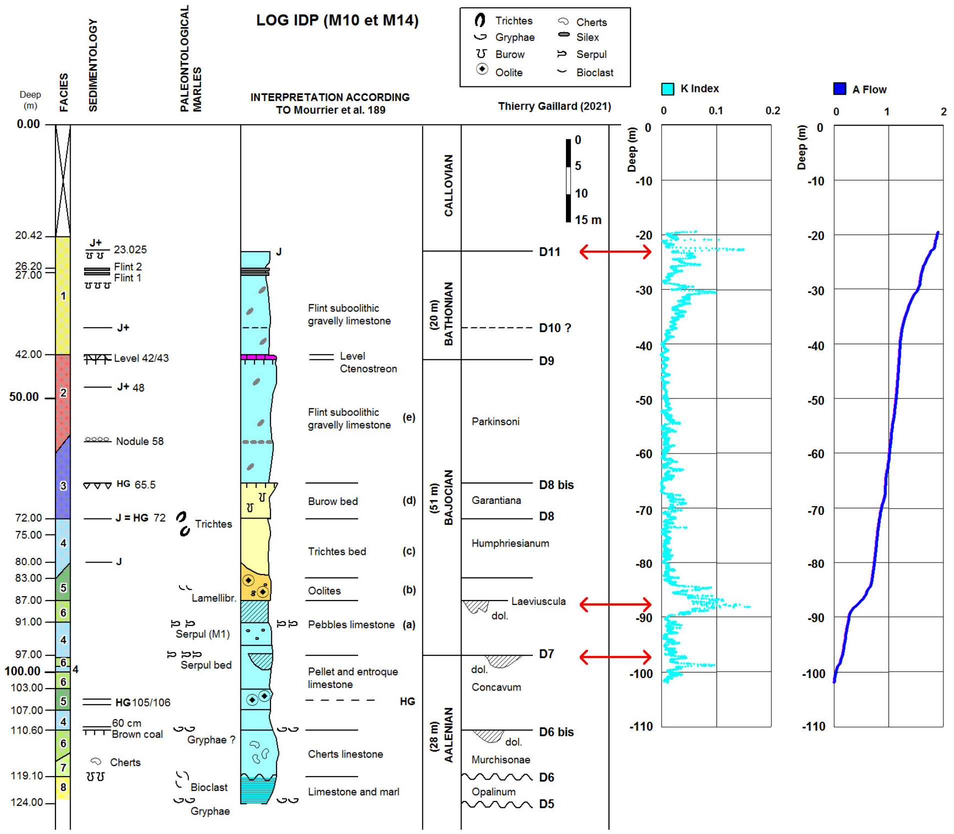

Fig. 8. Comparison of lithostratigraphic logs of M14, K-index, and A-Flow.

By extension, the search for these same correlations between lithostratigraphy and acoustic geophysics in boreholes C1, M11 and M20 allows us to propose the following summary table (cf. figure 8). The *Laeviuscula* discontinuity (stratigraphic boundary between the *Sowerbyi* biozone and the *Sauzei* biozone in the Bajocian) is systematically characterised and correlated between optical and acoustic imaging. The karst index was validated on all three boreholes (index not available on C1). For borehole M11, the karst characterisation index is high only at depths that correspond to discontinuities D6bis and *Laeviuscula*. Finally, for borehole M20, acoustic logging indicates the presence of karst at D7 and *Laeviuscula*. For boreholes M14, M11, and M20, a high karst index is calculated at depths correlated with the presence of a stratigraphic discontinuity.

Discontinuity	OPTV	acoustic section	K-index	OPTV caracterisation	acoustic section	K-index	OPTV	acoustic section	K-index	OPTV	acoustic section
	M14			M11			M20			C1	
D11	Yes	Yes	Yes								
D10	Yes	Yes	No								
D9	Yes	No	No								
D8bis	Yes	Yes	No	Yes	No	No					
D8	Yes	Yes	No	Yes	Yes	No	Yes	No	No	Yes	Yes
Laev.	Yes	Yes	Yes	Yes	Yes	Yes	Yes	Yes	Yes	Yes	Yes
D7	Yes	Yes	Yes	Yes	No	No	*Yes (probable)*	*Yes (probable)*	Yes	Yes	Yes
D6bis	Yes	Yes	No	Yes	Yes	Yes	Yes	No	No	Yes	Yes

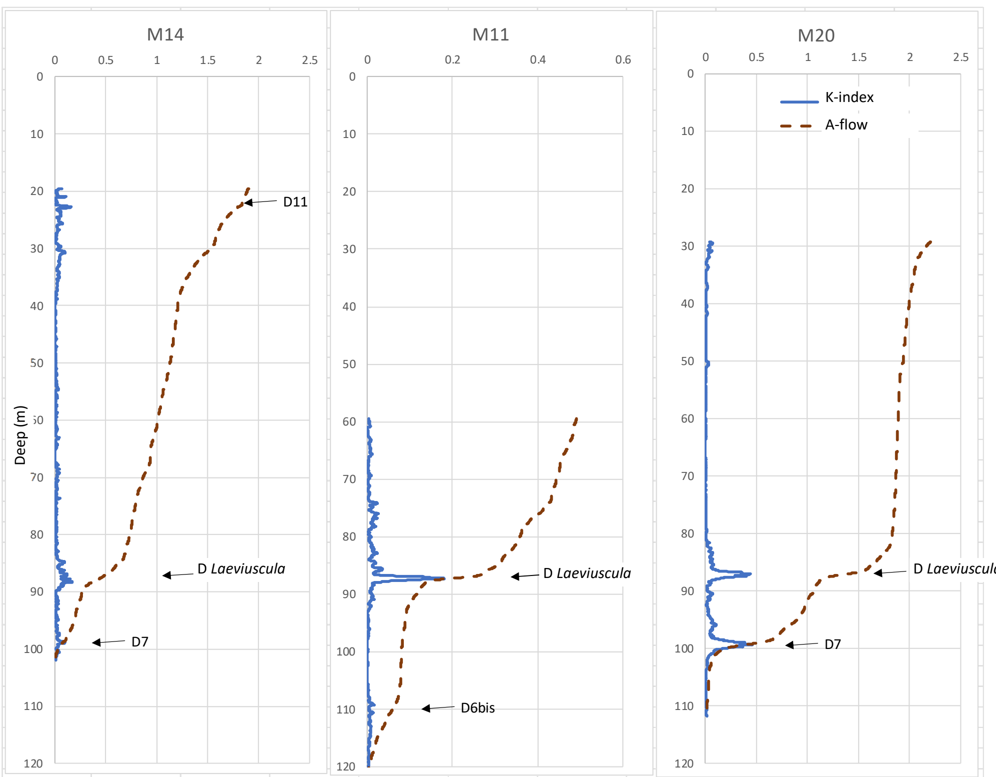

Fig. 9. Synthesis of stratigraphic discontinuity characterisation using optical (OPTV) and acoustic logging (K-index (blue curve), A-flow (dotted curve)).

Conclusion

The authors sought to understand the origin of horizontal karstic horizons revealed by geophysical investigations.

A 3-D seismic survey was designed to obtain a deep 3-D block with a broad horizontal extent. Structural interpretation of the 3D block led to the conclusion that the stratigraphy is nearly horizontal with a dip of 1 degree to the west. Consequently, no tectonic features with vertical displacement are present.

The 3D seismic block was converted into a 3-D pseudo-velocity block using acoustic velocity logs as constraints and then into a pseudo-porosity block which revealed three high-porosity, presumably water-producing layers at depths of 35-40, 85-87 and 110-115 m, identified as karstic horizons. The karstic horizons observed on the 3D seismic block were confirmed by both acoustic logging and borehole wall imaging with optical televiewer (OPTV). Regarding acoustic logging, a specific attribute, named the *K-index*, was computed to detect karstic bodies. However, K-index acoustic logs and optical televiewer data detected karstic bodies not detected by the 3D seismic method due the difference in vertical resolution between the seismic data (several meters) and logging data (several centimetres to several tens of centimetres).

The authors have shown that 3D seismic makes it possible to build a large-scale structural model that highlights karstic horizons that must be confirmed at borehole locations by very high-resolution geophysical tools, such as full waveform acoustic logging and OPTV logging. Then, by correlating karstic horizons with stratigraphy, the discontinuities that promote the formation of karstic horizons can be identified. The data acquired can be used to propose a new karstification model that is constrained by stratigraphy.

The authors have demonstrated that karstic horizons in the Dogger limestone at the SHE/HES site are closely related to stratigraphic discontinuities. As a result, the Dogger limestone aquifer at Poitou is composed of multiple productive horizons. These horizons can naturally communicate through fault and joint systems. However, in general, the drilling was conducted in such a way as to capture all karst horizons. The boreholes conducted in this manner therefore mix waters that have different pressures and chemical qualities. These water wells are thus particularly vulnerable to surface pollution and are capable of contaminating deeper karst formations. Each borehole must then undergo a lithological and paleontological description to study the key role of stratigraphy in the distribution of water inflows. This work assumes that well logging should be conducted before equipment and completion, including flow, gamma-ray, optical-televiewers, and other logging methods. Well geophysical tools should also be used to locate the karst horizons.

On the Poitou threshold, the proposed karstification model has several practical implications.

Once the large-scale structural model has been established and karst horizons identified, the first recommendation is to obtain optical televiewer data in all available boreholes to recalibrate stratigraphy and accurately locate karstic horizons.

The second recommendation is to consider screening each karstic horizon with appropriate boreholes. This will make it possible to both evaluate groundwater quality and vulnerability and to define borehole completions.

Deep karst is a well-protected resource for future generations.

Competing interest

The authors declare that they have no known competing financial interests or personal relationships that could have appeared to influence the work reported in this paper.

Acknowledgements

The authors thanks Benoit Nauleau for the assistance on HES, Pierre Gaudiani for the acquisition of acoustic data, Patricia Bobeck for the review of the English, and Valérie Monange for the drawing.

References

[1] P. Bernard, “La conquête de l'eau potable à Poitiers,” Travaux du Centre de Géographie Humaine et Sociale de l'Université de Poitiers, 1987.

[2] J. Welsch, “Hydrologie souterraine du Poitou calcaire,” *Spelunca,* no. 69, p. 70, 1922.

[3] J. Mari et G. Porel, «3D seismic imaging of a near – surface heterogeneous aquifer: a case study,» *Oil and Gas Science and Technology, Rev IFP63,* vol. 63, n° %12, pp. 179-201, 2008.

[4] F. Delay, J. Mari, G. Porel, F. Chabaux and P. Ackerer, “Is subsurface geophysics as seismic and acoustic investigations a rescue to groundwater flow inversion?,” *Comptes Rendus Geoscience de l'Académie des Sciences,* vol. 355, no. 1, pp. 1-20, 2022.

[5] J. Mari, G. Porel and F. Delay, “Contribution of Full Wave Acoustic Logging to the Detection and Prediction of Karstic Bodies,” *Water,* vol. 12, no. 4, p. 948, 2020.

[6] J. Mari and G. Porel, “Automated karstic reservoir analysis utilizing attributes,” in *77th EAGE Conference & Exhibition, Madrid IFEMA, Spain, 1-4 June*, Madrid, 2015.

[7] J. Gabilly, “Les variations de sédimentations du Lias et du Jurassique en relation avec le seuil du Poitou,” Poitiers, 1962.

[8] J. Gabilly et E. Cariou, «Groupe Français d'études du Jurassique : Journée d'études et excursion en Poitou 14-15-16 et 17 octobres 1974. Livret guide,» University of Poitiers, 1974.

[9] C. Gonnin, E. Cariou and P. Branger, “Les facteurs de contrôle de la sédimentation au début du Jurassique moyen sur le seuil du Poitou et ses abords,” *Compte Rendu de l'Académie des Sciences,* vol. 135, no. Série II, pp. 853-859, 1992.

[10] J. Gabilly and M. Rioult, “Le Bajocien inférieur et le Toarcien supérieur sur les bordures du Massif Armoricain,” in *Deuxième colloque du Jurassique*, Mémoire BRGM n°75, 1971, pp. 385-396.

[11] J. Welsh, “Sur la succession des faunes du Lias et du Bajocien inférieur dans le détroit du Poitou,” *Compte-Rendu de l'Académie des Sciences,* vol. 1, no. CXX, pp. 1291-1295, 1895.

[12] G. Beaulieu, “Etude géologique des terrains jurassiques dans la région de Lusignan, Montreuil-Bonnin et Latillé (stratigraphie, cartographie et structure).,” PhD thesis, University of Poitiers, 1978.

[13] B. Benvel, “Etude stratigraphique, sédimentologique et structurale du Jurassique dans les vallées du Clain et de la Boivre en amont de Poitiers,” PhD thesis, University of Poitiers, 1978.

[14] P. Branger, “La marge nord-Aquitaine et le seuil du Poitou au Bajocien : stratigraphie séquentielle, évolution biosédimentaire et paléogéographie,” PhD thesis, University of Poitiers, 1989.

[15] J.-P. Mourrier, “Le versant Parisien du seuil du Poitou de l'Hettangien au Bathonien. Stratigraphie, sédimentologie, caractères paléontologiques, Paleogéographie.,” PhD thesis University of Poitiers, 1983.

[16] J. Gabilly, E. Cariou and P. Hantzpergue, “Les grandes discontinuités du Jurassique : témoins d'évènements eustatiques, biologiques et sédimentaires,” *Bulletin de la Société Géologique de France,* vol. I, no. 3, pp. 391-401, 1985.

[17] C. Mangold, S. Ferri and J. Gabilly, “Les faunes du Bathonien dans la moitié sud de la France - Essai de corrélation,” *Colloque du Jurassique, Luxembourg,* pp. 103-109, 1967.

[18] E. Cariou and P. Hantzpergue, Biostratigraphie du Jurassique ouest-européen et méditérannéen : zonations parallèles et distribution des invertébrés et microfossiles, vol. 17, Groupe Français d'Etude du Jurassique-Elf-Aquitaine, 1997, p. 425.

[19] J. Gabilly, Guides géologiques régionaux : Poitou Charentes Vendée, avec la collaboration de Brillanceau A., Cariou E., Ducloux J., Dupuis J., Hantzpergue P., Moreau P., Santallier P., Ters M.,, Masson, 1978, p. 200.

[20] C. Gonnin, E. Cariou and P. Branger, “Stratigraphie séquentielle des séries du Bajocien inférieur au Bathonien moyen du seuil du Poitou et de son versant aquitain (France),” *C. R. Acad. Sci. Paris,,* vol. 316, no. H, pp. 209-215, 1993.

[21] F. Gaumet, M. Guitton and J.-P. Callot, “Hétérogénéité sédimentaire et fracturation dans le Jurassique du Site Expérimental Hydrogéologique de Poitiers,” 2004.